IEEE Access
Multidisciplinary | Rapid Review | Open Access Journal

Received November 12, 2018, accepted January 30, 2019, date of publication March 5, 2019, date of current version March 29, 2019.

Digital Object Identifier 10.1109/ACCESS.2019.2903089

Effects of Structure Parameters on Abnormal Opening of Pilot-Operated Relief Valve Under Alternating Pressure

QIANHUA HAO[1,2], WANRONG WU[1], XIANGJING LIANG[1], AND ZHI LIU[1]
[1]College of Mechanical and Electrical Engineering, Central South University, Changsha 410083, China
[2]School of Energy and Electromechanical, Hunan University of Humanities, Science and Technology, Loudi 417000, China

Corresponding author: Wanrong Wu (wwr@csu.edu.cn)

This work was supported in part by the National Natural Science Foundation of China under Grant 51774340, in part by the Hunan Provincial Natural Science Foundation of China under Grant 2019JJ50284, and in part by the Research Program of State Key Laboratory of High Performance Complex Manufacturing under Grant zzyjkt201503.

ABSTRACT Hydraulic vibration excitation has been widely regarded as a promising method of excitation because of its high power density and large output force. However, the alternating pressure in the hydraulic vibration exciter could cause the pilot-operated relief valve (PRV) to open abnormally, which presents a new challenge to the normal operation of the PRV. To determine the abnormal opening characteristics of the PRV under alternating pressure, the effects of structure parameters of the PRV (including diameters of orifices 1 and 2, volume of the pilot valve inlet, volume of the main valve spring chamber, area ratio of the main spool, and main spring pre-compression force and stiffness) on its abnormal opening displacement under alternating pressure were numerically investigated. The calculation results indicate that the abnormal opening of the PRV will be effectively decreased by appropriately increasing the diameter of orifice 1, decreasing the pilot valve inlet and main valve spring chamber volumes, and increasing the area ratio of the main spool and the main spring pre-compression force. The influence of the orifice 2 diameter on the abnormal opening of the PRV is dependent on the diameter range of orifice 1. The reasonable diameters of orifices 1 and 2 are in the range of 0.8–1.2 mm. The influence of the main valve spring chamber volume is more significant than the pilot valve inlet volume. The influence of the main spring stiffness is not significant.

INDEX TERMS Alternating pressure, pilot-operated relief valve, abnormal opening, effects of structure parameters, hydraulic vibration excitation.

I. INTRODUCTION

Hydraulic vibration excitation (HVE) has been widely regarded as a promising method of excitation because of its high power density and large output force [1]–[4]. However, the HVE working pressure inevitably varies alternately during the excitation process, which could cause instability in the hydraulic system and components [5]. As the most commonly used overload protection component in hydraulic systems, the pilot-operated relief valve (PRV) can be opened abnormally under alternating pressure [6]. This abnormal opening means that, although the system pressure is significantly lower than the pressure setting of the PRV, the main valve is periodically opened. The abnormal opening of the PRV not only increases the energy loss through discharging the flow rate, but also shortens its service life by increasing the friction between the main spool and the seat. Numerous studies have reported the fundamental characteristics of the PRV [7]–[10], and pressure fluctuations [11], [12]. However, abnormal opening of the PRV has received minimal attention. Therefore, more studies on the effect mechanism of the abnormal opening of the PRV under alternating pressure should be conducted.

Previously, a number of scholars had made important contributions to understanding the abnormal opening of the PRV. Dimitrov [13] reported that the main spool was moved before the pilot spool during the dynamic response of the PRV, and a PRV with a compensation piston was proposed to improve the phenomenon. However, the normal operation of the valve was limited by the diameter of the compensating piston, which could cause the valve to be unstable. Wu *et al.* [6] reported the abnormal opening of the PRV under alternating pressure, but the effects of its structure parameters were not

The associate editor coordinating the review of this manuscript and approving it for publication was Tao Wang.

discussed in detail. From the above, it can be concluded that the abnormal opening occurs during the dynamic response of the PRV. To further improve the general performance of the PRV, the relationship between its structure parameters and dynamic performance has received increasing attention in recent years. Dasgupta and Watton [14] found that the diameters of orifices 1 and 2 both have an important influence on the transient response of the valve. Shin [15] reported the influence of some structure parameters on the dynamic characteristics of the Vickers type PRV, including the main spring stiffness. Nakanishi *et al.* [16] reported the relationship between some structure parameters of the PRV and its stability, including the main valve spring chamber volume. Deng and Liu [17] investigated the effects of some structure parameters on the dynamic response performance of a giant forging hydraulic press. The above results indicated that the structure parameters of the PRV are critical to its dynamic performance. Apart from its structure parameters, a number of relief valves with special structures have also been reported by several scholars [18]–[20].

From the abovementioned studies, the abnormal opening of the PRV occurs in its dynamic response process, and its dynamic response characteristics are closely related to the structure parameters of the valve. However, systematic and in-depth investigations are still rare. The aim of this study is to investigate the effects of PRV structure parameters on abnormal opening under alternating pressure and provide a theoretical basis for the design and optimization of the valve. The maximum opening displacement of the main spool is utilized to characterize the abnormal opening degree. The influence of seven basic structure parameters on the maximum opening displacement of the main spool is numerically investigated.

II. DESCRIPTION OF PRV

Figure 1 shows a schematic diagram of the PRV. In the initial state the main valve is closed, because the pressures in the main valve inlet, the main valve spring chamber, and the pilot valve inlet are equal. The pilot valve will be opened when the force, produced by the pressure in the pilot valve inlet on the pilot spool, is greater than the pilot spring pre-compression force. The oil in the main valve inlet will flow through the orifice 1 and flow out from the pilot valve. Because of the effect of orifice 1, there will be a pressure drop between the upper and lower chambers of the main spool. When the force produced by the pressure drop on the main spool is sufficient to overcome the main spring pre-compression force, the main spool will be pushed upward and begin to overflow. The pilot valve will be closed when the pilot spring pre-compression force is greater than the force generated by the pressure in the pilot valve inlet on the pilot spool. At this time, there is no flow rate through the orifice 1, so the main valve is closed. Clearly, when the PRV is abnormally opened, the pilot valve is always closed because the force, exerted by the pressure in the pilot valve inlet on the pilot spool, is less than the pilot spring pre-compression force.

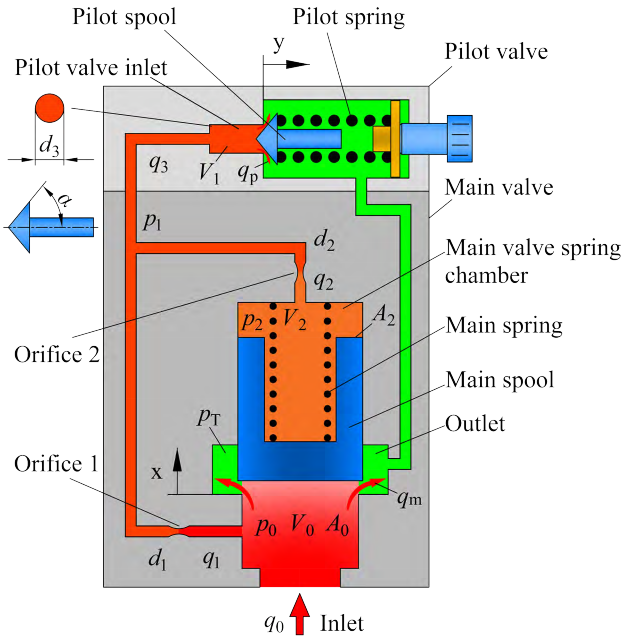

FIGURE 1. Schematic diagram of PRV.

The opening condition of the main valve in the PRV is

$$p_0 A_0 > p_2 A_2 + k_x x_0 + m_0 g + F_f \tag{1}$$

where p_0 is the pressure in the main valve inlet, p_2 is the pressure in the main valve spring chamber, A_0 and A_2 are the effective areas of the lower and upper ends of the main spool, respectively, k_x and x_0 are the main spring stiffness and its pre-compression displacement, respectively, m_0 is the mass of the main spool, and F_f is the static friction between the main spool and the seat.

Compared to the main spring pre-compression force, both the gravity of the main spool and the static friction between the main spool and the seat are insignificant, and can be ignored. Therefore, Equation (1) can be simplified as follows:

$$p_0 - \lambda p_2 > \frac{F_{x0}}{A_0} \tag{2}$$

$$\lambda = A_2 / A_0 \tag{3}$$

$$F_{x0} = k_x x_0 \tag{4}$$

where λ is the area ratio of the main spool, and F_{x0} is the main spring pre-compression force.

III. DESCRIPTION OF MODELS AND METHODOLOGY

A. MATHEMATICAL MODEL OF PRV

The following assumptions are accepted in the mathematical model describing the abnormal opening process of the PRV [21]–[23].

(1) The mass of the spool and spring is negligible.

(2) The effects of coulomb friction and flow force are ignored.

(3) The leakage of the PRV is negligible.

(4) The reservoir pressure is assumed to be atmospheric and can be neglected ($p_T = 0$ Pa).

According to Newton's second law and the actual force acting on the main spool, the force balance equation of the main spool can be described as follows:

$$p_0A_0 - p_2A_2 = m_0\frac{d^2x}{dt^2} + B_0\frac{dx}{dt} + k_x(x_0 + x) \tag{5}$$

where B_0 is the viscous damping coefficient of the main spool, and x is the displacement of the main spool.

The continuity equation of the flow rate in the main valve inlet can be expressed as follows:

$$q_0 = \frac{V_0}{\beta}\frac{dp_0}{dt} + A_0\frac{dx}{dt} + q_m + q_1 \tag{6}$$

where q_0 is the flow rate through the main valve inlet, V_0 is the volume of the main valve inlet, β is the oil bulk modulus, q_m is the flow rate through the main valve outlet, and q_1 is the flow rate through the orifice 1.

The flow rate through the main valve outlet is given by

$$q_m = C_{d,m}A_x\sqrt{\frac{2}{\rho}(p_0 - p_T)} \tag{7}$$

where p_T is the pressure in the main valve outlet, $C_{d,m}$ is the discharge coefficient of the main valve outlet, ρ is the oil density, and A_x is the flow area of the main valve outlet which can be obtained by

$$A_x = n\left[\frac{d_0^2}{4}\cos^{-1}(1 - \frac{2x}{d_0}) - (\frac{d_0}{2} - x)\sqrt{x(d_0 - x)}\right] \tag{8}$$

where n is the number of drain holes on the main valve sleeve, and d_0 is the diameter of the drain hole on the main valve sleeve.

The flow rate through the orifice 1 is given by

$$q_1 = C_{d,1}\frac{\pi d_1^2}{4}\sqrt{\frac{2}{\rho}(p_0 - p_1)sign(p_0 - p_1)} \tag{9}$$

where $C_{d,1}$ is the discharge coefficient of orifice 1, d_1 is the diameter of orifice 1, and p_1 is the pressure in the pilot valve inlet.

The continuity equation of flow rate in the main valve spring chamber can be described as follows:

$$q_2 = (\frac{V_2}{\beta}\frac{dp_2}{dt} - A_2\frac{dx}{dt})sign(\Delta p_{12}) \tag{10}$$

$$\Delta p_{12} = p_1 - p_2 \tag{11}$$

where q_2 is the flow rate through the orifice 2, V_2 is the volume of the main valve spring chamber, and Δp_{12} is the pressure drop across the orifice 2.

The flow rate through the orifice 2 is given by

$$q_2 = C_{d,2}\frac{\pi d_2^2}{4}\sqrt{\frac{2}{\rho}\Delta p_{12}sign(\Delta p_{12})} \tag{12}$$

where $C_{d,2}$ is the discharge coefficient of orifice 2, and d_2 is the diameter of orifice 2.

The force balance equation of the pilot spool can be described as follows:

$$p_1\frac{\pi d_3^2}{4} = m_1\frac{d^2y}{dt^2} + B_1sign(\frac{dy}{dt}) + k_y(y_0 + y) \tag{13}$$

where d_3 is the diameter of the orifice in pilot valve seat, m_1 is the mass of the pilot spool, B_1 is the viscous damping coefficient of the pilot spool, k_y and y_0 are the pilot spring stiffness and its pre-compression displacement, respectively, and y is the displacement of the pilot spool.

The continuity equation of the flow rate in the pilot valve inlet can be expressed as follows:

$$q_1 = \frac{V_1}{\beta}\frac{dp_1}{dt} + q_p + q_2sign(\Delta p_{12}) \tag{14}$$

where V_1 is the volume of the pilot valve inlet, and q_p is the flow rate through the pilot valve outlet.

The flow rate through the pilot valve outlet is given by

$$q_p = C_{d,p}\pi d_3 y\sin\alpha\sqrt{\frac{2}{\rho}(p_1 - p_T)} \tag{15}$$

where $C_{d,p}$ is the discharge coefficient of the pilot valve port, and α is the half cone angle of the pilot spool.

B. SIMULATION METHOD AND SETTINGS

1) SIMULATION METHOD

The MATLAB/Simulink® package is used for the modeling of Eqs. (5)–(15), and the simulation model of the PRV is shown in Fig. 2. The Runge–Kutta fourth-order method is used as the solver. The time step for the calculations is fixed at 0.1 μs.

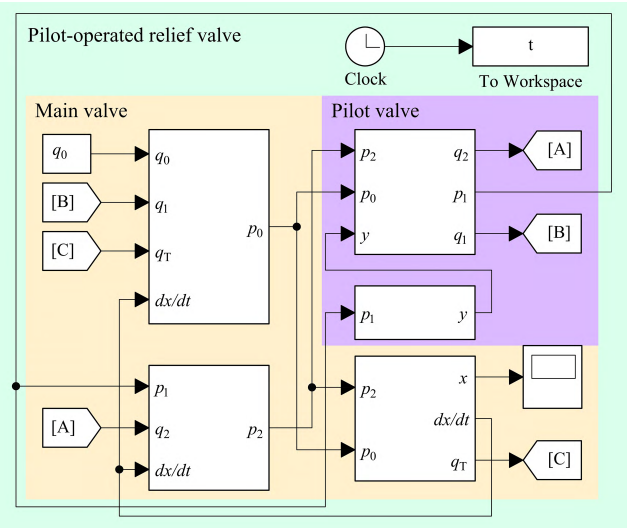

FIGURE 2. Simulation model of PRV.

2) SIMULATION PARAMETER SETTING

Table 1 presents the complete list of parameters used in the simulation, the bulk of which are obtained by actual measurements, and others are estimated empirically. As the pilot valve

TABLE 1. List of simulation parameters.

Parameters	Value	Parameters	Value
m_0	0.06 kg	d_0	7.5 mm
d_1	0.4 ~ 1.6 mm	d_2	0.4 ~ 1.6 mm
F_{x0}	0 ~ 170 N	V_0	1400 ml
V_1	2 ~ 10 ml	V_2	2 ~ 10 ml
λ	1.02 ~ 1.06	A_2	452.16 mm^2
k_x	10 ~ 30 N/mm	k_y	30 N/mm
B_0	100 Ns/m	B_1	35 Ns/m
q_0	10 L/min	n	8
m_1	0.02 kg	p_T	0 Pa
$C_{d,1}$	0.6	$C_{d,2}$	0.6
$C_{d,m}$	0.6	$C_{d,p}$	0.6
d_3	4 mm	α	30°
B	1000 MPa	ρ	850 kg/m^3

is not opened when the main valve is abnormally opened, the pilot spring pre-compression force is set to infinity during the simulation for the abnormal opening of the PRV.

3) STRUCTURE PARAMETERS FOR ANALYSIS

Based on the above, the following structure parameters are used for the analysis: diameter of orifice 1 (d_1), diameter of orifice 2 (d_2), volume of the pilot valve inlet (V_1), volume of the main valve spring chamber (V_2), area ratio of the main spool (λ), main spring pre-compression force (F_{x0}), and main spring stiffness (k_x).

The first four and the last parameters were selected based on previous studies [14]–[17], [21]. These studies reported that they are related to the dynamic response of the PRV. The area ratio λ is defined by changing the effective area of the lower-end of the main spool (A_0), while the effective area of the upper-end of the main spool (A_2) remains constant. Parameter F_{x0} is selected because it affects the force acting on the main spool. The mass of the main spool (m_0) cannot be significantly varied because of geometrical and dimensional limitations of the PRV, and is not included in the analysis in this study.

4) DESCRIPTION OF ALTERNATING PRESSURE

The actual measured pressure in the inlet of the PRV during hydraulic excitation is shown in Fig. 3(a). As can be seen, the inlet pressure alternates periodically and the pressure waveform presents triangular wave characteristics. Therefore, in the simulation for the abnormal opening of the PRV, the inlet pressure is characterized by a triangular wave, as shown in Fig. 3(b), where the pressure peak p_p is 8 MPa, the pressure amplitude p_m is 5 MPa, and the pressure gradient p_k is 2 MPa/ms.

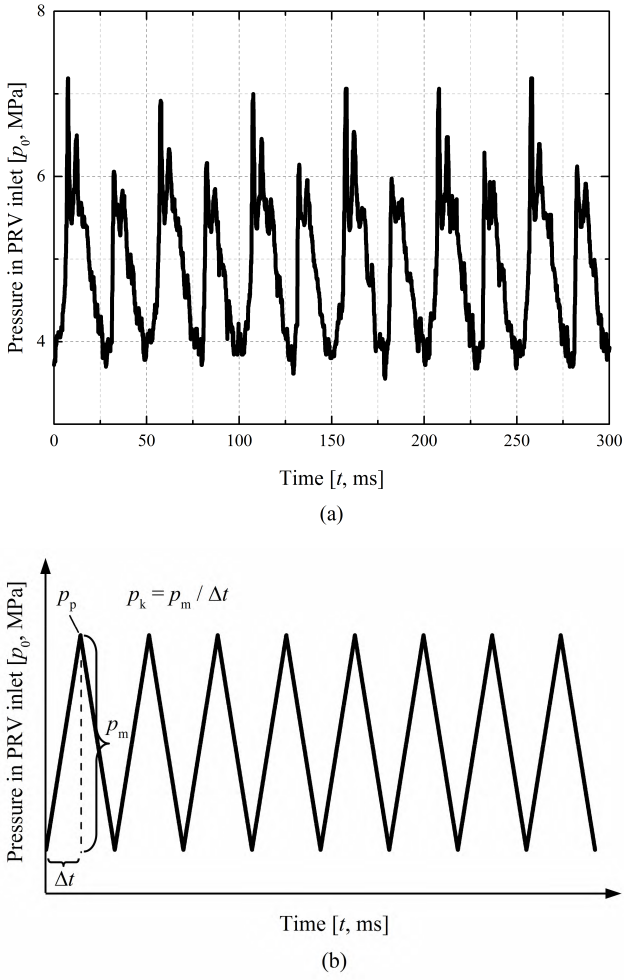

FIGURE 3. Pressure in PRV inlet: (a) experimental values, and (b) equivalent values.

C. CALCULATION RESULTS AND MODEL VALIDATION

To verify the accuracy of the adopted model, the calculation data should be verified by experimental results. As it is the critical indicator reflecting the dynamic response characteristics of the PRV, the inlet pressure p_0 was verified at a step flow rate. The validation experiments were conducted on the PRV performance test bench, which is shown in Fig. 4.

Figure 5 shows the inlet pressure p_0 comparison between the calculated data and the experimental results. As can be seen, the simulated p_0 is in good agreement with the experimental p_0, and the maximum relative error is approximately 11.8% (at 22 ms). The maximum overshoot ratios of the simulated and experimental p_0, 6.06% and 5.26%, respectively, are also in good agreement. Therefore, the simulation data is in good agreement with the experimental results, and the established simulation model can be regarded as scientific and reasonable.

IV. RESULTS AND DISCUSSIONS

A. INFLUENCE OF ORIFICE 1 DIAMETER

The diameter of orifice 1, which acts to create a pressure drop between the main valve inlet and the pilot valve inlet, is a

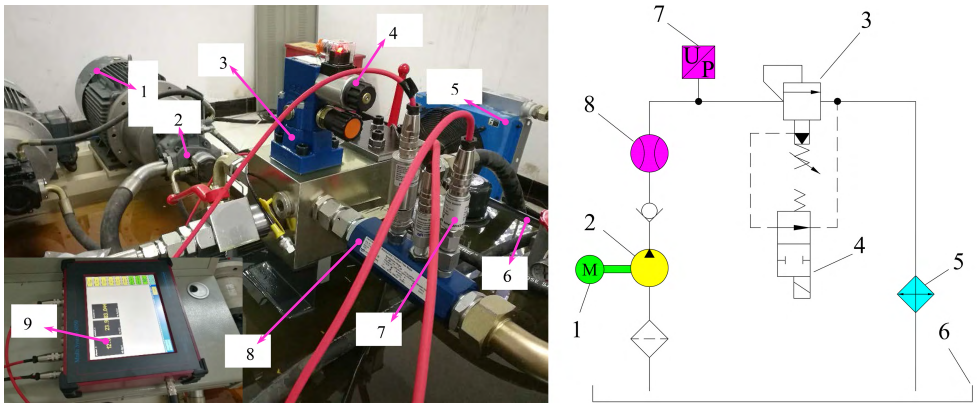

FIGURE 4. PRV test setup: 1- Electric motor; 2- Pump; 3- PRV; 4- 2/2 Solenoid directional valve; 5- Radiator; 6- Oil tank; 7- Pressure sensor; 8- Flow meter; and 9- Hydrotechnik 8050 measuring instrument.

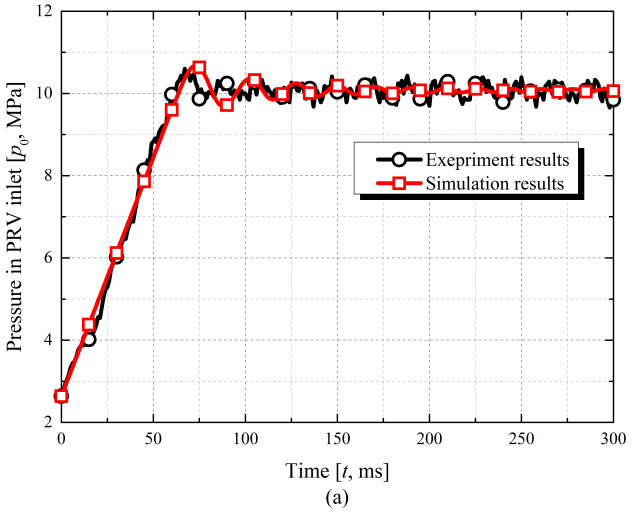

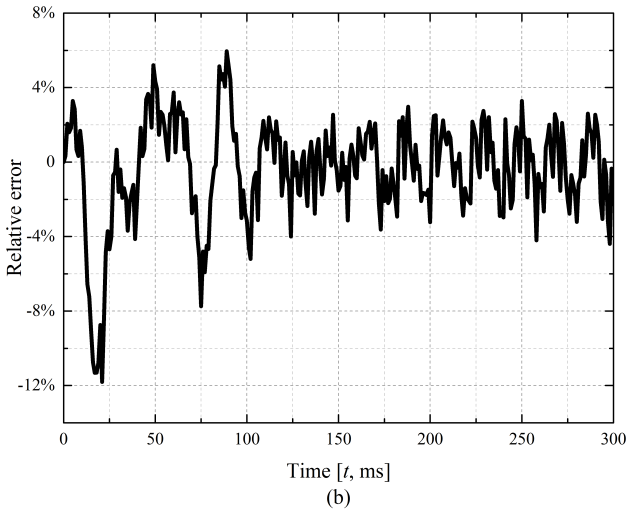

FIGURE 5. Comparison of p_0 between simulation and experimental results: (a) absolute values, and (b) relative error.

critical PRV parameter. Thirteen diameter values for orifice 1 (d_1, from 0.4 mm to 1.6 mm) were investigated in this study. To avoid accidental results, six diameter values for orifice 2

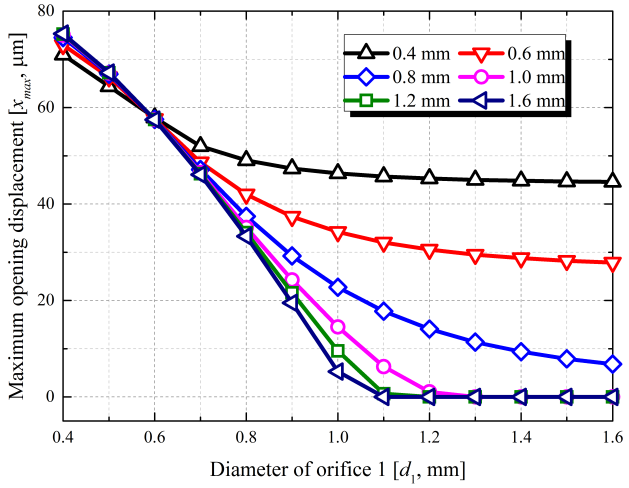

FIGURE 6. Variation of x_{max} with increase of d_1 under different d_2.

(d_2, from 0.4 mm to 1.6 mm) were used. All other structure parameters were the same as presented in Table 1.

Figure 6 shows the variation in the maximum abnormal opening displacement of the main spool (x_{max}) with increasing orifice 1 diameter. As can be seen, with increasing d_1, x_{max} monotonously decreases and tends toward convergence. The maximum decrease is 75.3 μm ($d_2 = 1.6$ mm), and the minimum is 35.4 μm ($d_2 = 0.4$ mm).

In fact, with increasing d_1, the oil in the main valve inlet will flow more easily into the pilot valve inlet. It will promote an increase in the pressure build-up rate in the pilot valve inlet, and induce an increase in the pressure difference (Δp_{12}) between the pilot valve inlet and the main valve spring chamber, which is also the pressure drop across orifice 2, as shown in Fig. 7. The greater Δp_{12} will promote an increase in the flow rate through orifice 2 into the main valve spring chamber, which will cause the rise of the pressure in the main valve spring chamber (p_2). The increased p_2 will result in a decrease in x_{max}. However, if d_1 is greater than 1.2 mm, the effects of reducing x_{max} by further increasing d_1 will not be significant. This is because Δp_{12} saturates when d_1 exceeds 1.2 mm, as can be seen in Fig. 7.

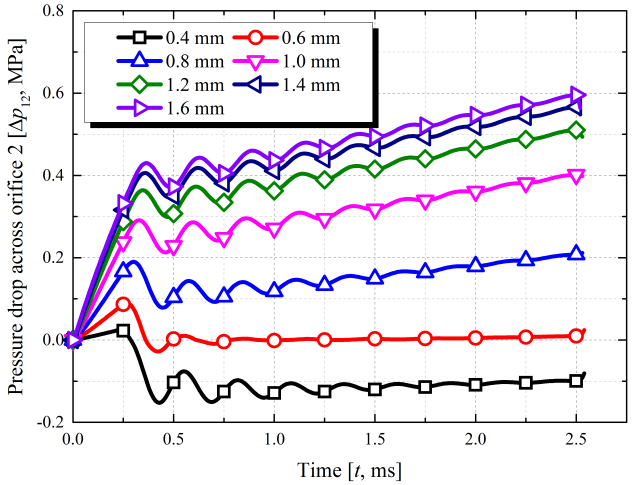

FIGURE 7. Pressure drop across orifice 2 under different d_1.

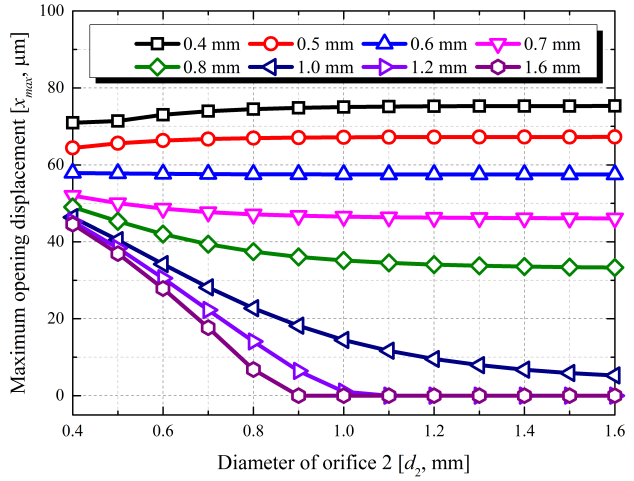

FIGURE 8. Variation of x_{max} with increasing d_2.

Figure 6 also shows that the different orifice 2 diameters affect the gradient of the abnormal opening degree with the diameter of orifice 1, but they do not affect the trend.

Based on the above, increasing d_1 is a better way to reduce the maximum abnormal opening displacement of the main spool. However, it is not necessary for d_1 to be greater than 1.2 mm.

B. INFLUENCE OF ORIFICE 2 DIAMETER

The diameter of orifice 2 is also a critical PRV parameter. As for orifice 1, thirteen diameter values for orifice 2 (d_2, from 0.4 mm to 1.6 mm) were investigated in this study. To investigate the coupling effect of orifice 1, eight diameter values for orifice 1 (d_1, from 0.4 mm to 1.6 mm) were used.

Figure 8 shows the variation in the maximum abnormal opening displacement of the main spool (x_{max}) with increasing orifice 2 diameter. It can be seen that the influence of d_2 on the abnormal opening of the PRV is significantly affected by the coupling effect of d_1. When d_1 is greater than 0.8 mm, the increase in d_2 can significantly decrease the abnormal opening degree, and the maximum decrease is 44.6 μm. However, when d_1 is less than 0.6 mm, the enlarged d_2 will increase the abnormal opening degree. When d_1 is 0.6–0.8 mm, the effect of d_2 on the abnormal opening degree is insignificant.

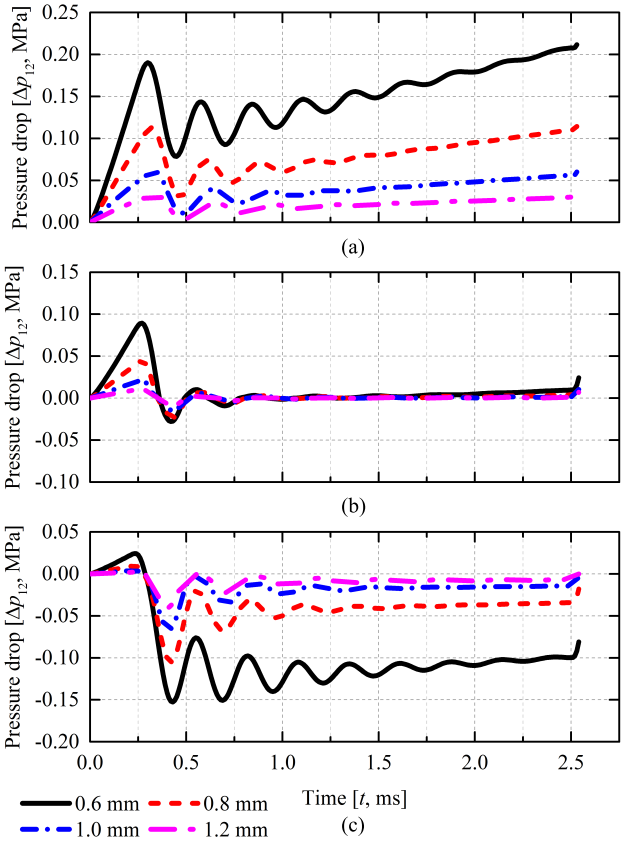

FIGURE 9. Pressure drop across orifice 2 under different d_1 and d_2. (a) d_1: 0.8 mm, (b) d_1: 0.6 mm, and (c) d_1: 0.4 mm.

This is because of the difference in pressure build-up rates in the pilot valve inlet and the main valve spring chamber. When d_1 is 0.8–1.6 mm, the oil in the main valve inlet can easily flow into the pilot valve inlet, therefore, the pressure build-up rate in the pilot valve inlet will be higher than the rate in the main valve spring chamber, which means that Δp_{12} will be greater than zero. Figure 9(a) shows an example with $d_1 = 0.8$ mm. As can be seen, the increased d_2 induces a significant decrease in Δp_{12}, which means that the oil in the pilot valve inlet will more easily flow into the main valve spring chamber to establish pressure, therefore, x_{max} can be significantly decreased. However, when d_1 is 0.4–0.6 mm, the oil in the main valve inlet will be difficult to flow into the pilot valve inlet, and the pressure in the pilot valve inlet increases very slowly. Therefore, the pressure build-up rate in the pilot valve inlet will be smaller than the rate in the main valve spring chamber, which means that Δp_{12} will be less than zero, as shown in Fig. 9(c) ($d_1 = 0.4$ mm). At this time, the increase in d_2 will cause the oil in the main valve spring chamber to flow easily into the pilot valve inlet, which will

increase x_{max}. When d_1 is 0.6–0.8 mm, the pressure build-up rate in the pilot valve inlet is essentially equal to the rate in the main valve spring chamber. Taking $d_1 = 0.6$ mm as an example, the pressure drop across orifice 2 is approximately zero, as shown in Fig. 9(b). Therefore, x_{max} will only change marginally.

According to Figs. 6 and 8, the ''normal operating area'', the ''slightly abnormal opening area'', and the ''severely abnormal opening area'' of the PRV under alternating pressure can be obtained when different d_1 and d_2 are combined, as shown in Fig. 10. The x_{max} is smaller than 40 μm in the ''slightly abnormal opening area'', and the x_{max} in the ''severely abnormal opening area'' is greater than 40 μm. The PRV in the ''normal operating area'' does not open abnormally, but excessive diameters of orifices 1 and 2 could cause the PRV to be difficult to open.

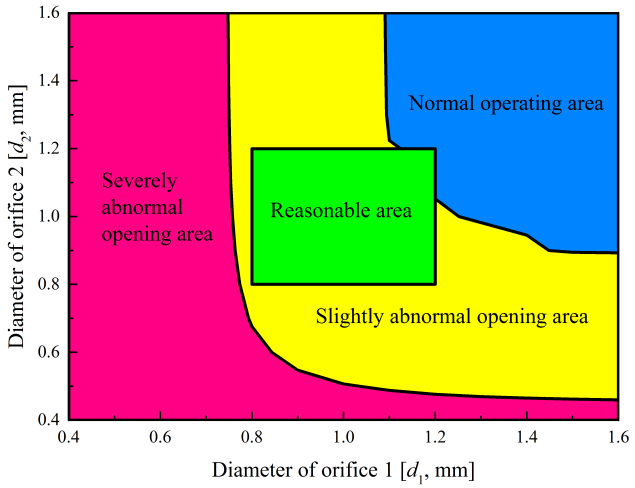

FIGURE 10. Working state of PRV when different d_1 and d_2 are combined.

Based on the above, a more reasonable diameter range, for both the orifices 1 and 2, should be 0.8–1.2 mm, as shown in Fig. 10.

C. INFLUENCE OF PILOT VALVE INLET VOLUME

Figure 11 shows the variation in the maximum abnormal opening displacement of the main spool (x_{max}) and its gradient (x'_{max}) with increasing pilot valve inlet volume (V_1). As can be seen, as V_1 increases, x_{max} monotonically increases with the trend of decelerating after acceleration, and the maximum increase is approximately 66.1 μm.

In fact, the increased V_1 will decrease the pressure build-up rate in the pilot valve inlet, which will decrease the flow rate through orifice 2 (q_2) into the main valve spring chamber, and could even change the direction of the flow. It will considerably decrease the pressure build-up rate in the main valve spring chamber and induce a significant increase in x_{max}. Figure 12 shows the pressure drop across orifice 2 under different V_1 during the main spool opening displacement from zero to x_{max}. This indicates that the above analysis for the effect mechanism of V_1 on x_{max} is correct.

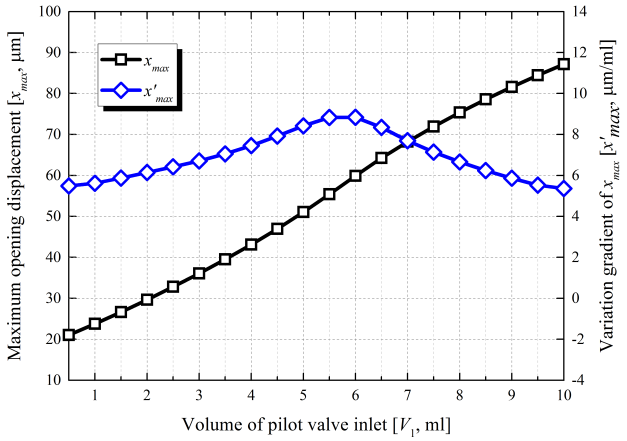

FIGURE 11. Variation of x_{max} and x'_{max} with increasing V_1.

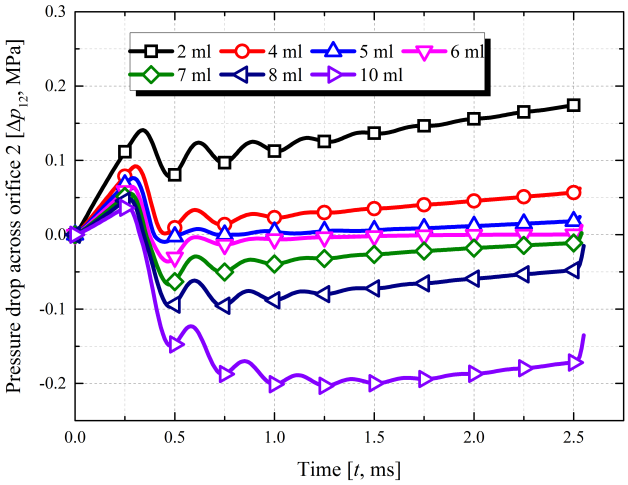

FIGURE 12. Pressure drop across orifice 2 under different V_1.

Figure 11 also shows that, when V_1 is approximately 6 ml, x_{max} is highly sensitive to changes in V_1, with a maximum gradient of 8.84 μm/ml ($V_1 = 6$ ml). This is because, when V_1 is 6 ml, Δp_{12} is approximately zero and q_2 is in a critical state of direction change.

Based on the above, to decrease the maximum abnormal opening displacement of the main spool, the volume of the pilot valve inlet should be reduced as much as possible.

D. INFLUENCE OF MAIN VALVE SPRING CHAMBER VOLUME

Figure 13 shows the variation in the maximum abnormal opening displacement of the main spool (x_{max}) and its gradient (x'_{max}) with increasing main valve spring chamber volume (V_2). As can be seen, the main valve port of the PRV will not be opened abnormally when V_2 is smaller than 2 ml, and x_{max} increases linearly with V_2 when V_2 exceeds 2 ml. The maximum increase is 74.9 μm.

This phenomenon is attributed to the pressure build-up rate in the main valve spring chamber (p_{k2}). Figure 14 shows the pressure build-up rate in the main valve spring chamber

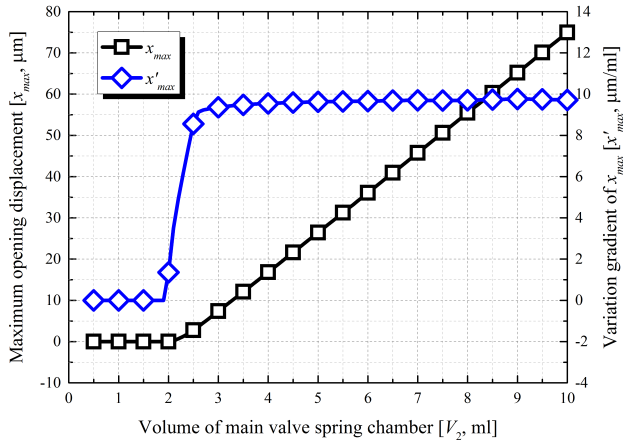

FIGURE 13. Variation of x_{max} and x'_{max} with increasing V_2.

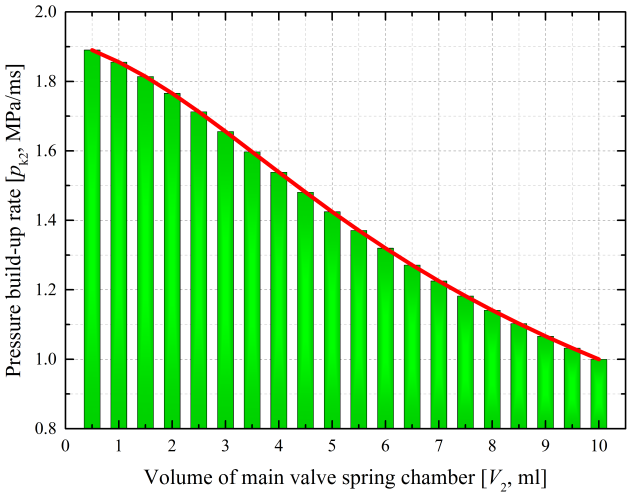

FIGURE 14. Variation of p_{k2} with increasing V_2.

under different V_2. As can be seen, with increasing V_2, p_{k2} will decrease from 1.9 MPa/ms to 1.0 MPa/ms, a decrease of 47.4%. Therefore, the increased V_2 directly decreases p_{k2}, which will induce a significant increase in x_{max}.

Comparing Fig. 11 with Fig. 13, it is observed that the gradient of x_{max} versus V_2 is greater than that of x_{max} versus V_1. Therefore, it can be concluded that V_2 has a more significant effect on the abnormal opening of the PRV than V_1, and this conclusion can also be obtained from the mathematical model in Section III. According to the above mathematical model, the Laplace transform ratio of p_2 and p_0 can be obtained as follows:

$$\frac{P_2}{P_0} = \frac{1}{(\frac{V_1}{\beta K_1} + \frac{V_2}{\beta K_1} + \frac{V_2}{\beta K_2})s + 1} \tag{16}$$

$$K_1 = \frac{\sqrt{2}}{8} C_{d,1} \pi d_1^2 (\rho\,|P_0 - P_1|)^{-\frac{1}{2}} \tag{17}$$

$$K_2 = \frac{\sqrt{2}}{8} C_{d,2} \pi d_2^2 (\rho\,|P_1 - P_2|)^{-\frac{1}{2}} \tag{18}$$

where P_0 and P_2 are the Laplace transforms of p_0 and p_2, respectively, and s is the Laplacian.

The response rate of p_2 to p_0 can be described by the time constant τ, which is given by

$$\tau = \frac{1}{\beta K_1}(V_1 + V_2 + V_2 \frac{K_1}{K_2}) \tag{19}$$

The partial derivatives of τ versus V_1 and V_2 can be described as follows, respectively:

$$\frac{\partial \tau}{\partial V_1} = \frac{1}{EK_1} \tag{20}$$

$$\frac{\partial \tau}{\partial V_2} = (\frac{1}{EK_1} + \frac{1}{EK_2}) \tag{21}$$

It is clear that the partial derivative of τ versus V_2 is greater than that versus V_1. Therefore, the same conclusion can be drawn.

Based on the above, to suppress the abnormal opening of the PRV under alternating pressure, V_2 should be reduced as much as possible, and decreasing V_2 should be given priority over V_1.

E. INFLUENCE OF MAIN SPOOL AREA RATIO

To reliably press the main spool against the seat, the upper-end area of the main spool (A_2) is typically marginally greater than its lower-end area (A_0), and the area ratio of the main spool (λ) is typically 1.02–1.06.

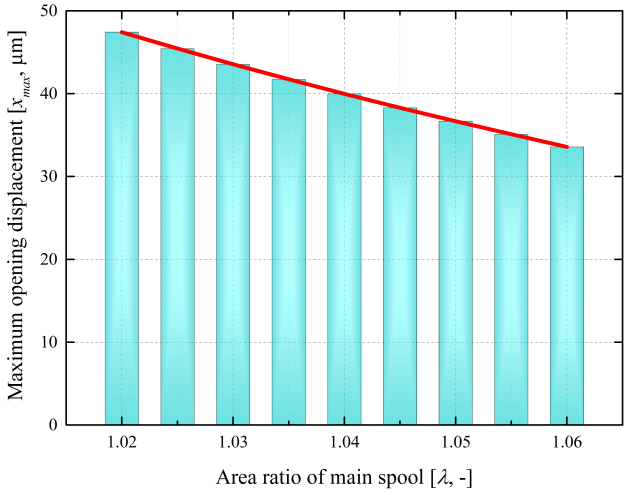

FIGURE 15. Variation of x_{max} with increasing λ.

Figure 15 shows the variation in the maximum abnormal opening displacement of the main spool (x_{max}) with increasing area ratio (λ). As can be seen, x_{max} decreases linearly as λ increases, and the maximum decrease is 13.8 μm.

This is because, when A_2 is constant, increasing λ means that A_0 will decrease, which will directly cause the force, produced by the pressure in the main valve inlet on the lower-end face of the main spool, to decrease during the abnormal opening of the valve. The decreased force will definitely cause x_{max} to decrease. However, as the variation range of λ is small, the effect of λ on x_{max} is not as significant as the four parameters analyzed above.

Based on the above, to decrease the maximum abnormal opening displacement of the main spool, the area ratio of the main spool can be increased in its available size range.

F. INFLUENCE OF MAIN SPRING PRE-COMPRESSION FORCE

Different main spring pre-compression forces are obtained by changing the pre-compression displacement (x_0) and maintaining the stiffness (k_x) constant during the simulation.

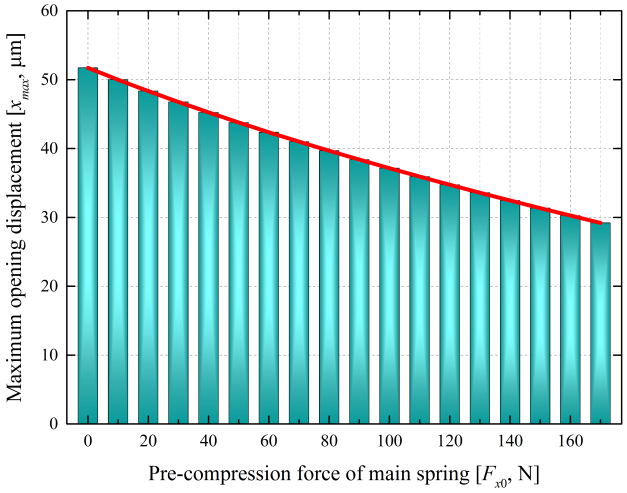

FIGURE 16. Variation of x_{max} with increasing F_{x0}.

Figure 16 shows the variation in the maximum abnormal opening displacement of the main spool (x_{max}) with increasing main spring pre-compression force (F_{x0}). As can be seen, with the increase of F_{x0} from 0 N to 170 N, x_{max} decreases linearly, and the maximum decrease is 22.5 μm.

This is because an increase in the main spring pre-compression force means that the force against the opening of the main spool increases. The increased resistance will clearly result in x_{max} decreasing. However, because of the structural constraints of the PRV, F_{x0} cannot be set too large, and excessive F_{x0} will also make the normal opening of the PRV difficult.

Based on the above analysis, it can be concluded that the maximum abnormal opening displacement of the main spool can be reduced by increasing the main spring pre-compression force, although the effect is limited.

G. INFLUENCE OF MAIN SPRING STIFFNESS

To independently analyze the effect of the main spring stiffness, the main spring pre-compression force is kept constant. Figure 17 shows the variation in the maximum abnormal opening displacement of the main spool (x_{max}) at a main spring stiffness of 10–30 N/mm. As can be seen, the main spring stiffness has little effect on the abnormal opening of the PRV.

This is attributed to the fact that the displacement of the main spool is negligible during the abnormal opening of the PRV, and the variation in the main spring force

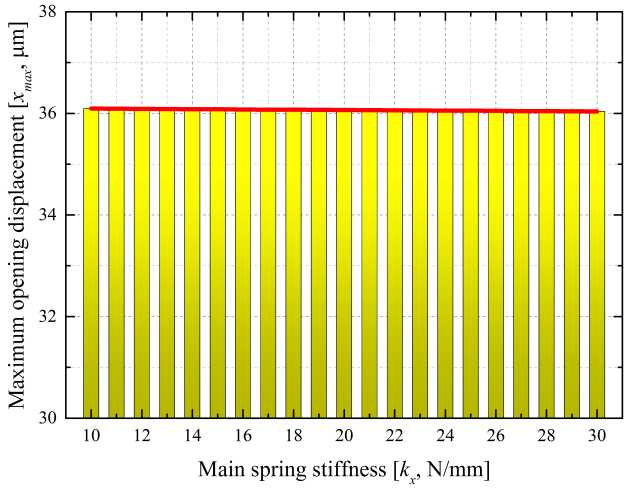

FIGURE 17. Variation of x_{max} with increasing k_x.

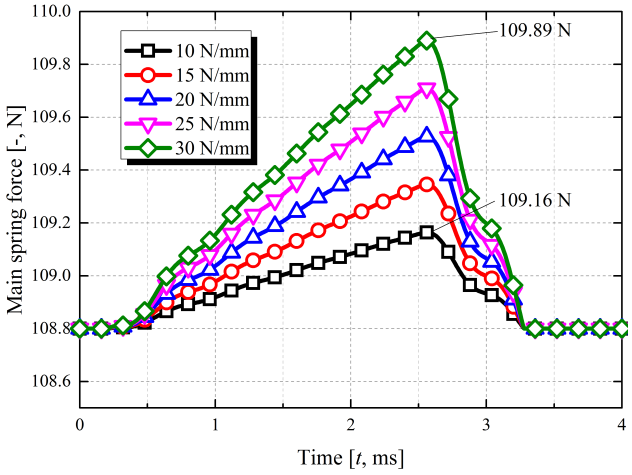

FIGURE 18. Variation of main spring forces.

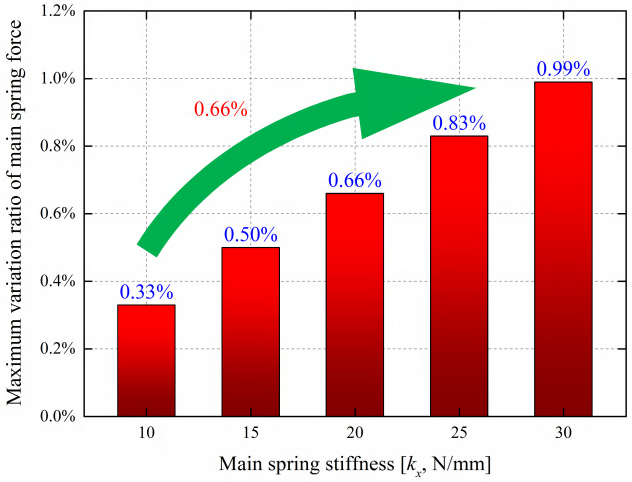

FIGURE 19. Maximum variation ratio of spring force under different k_x.

is also too small to cause a significant variation in x_{max}. When the main spring stiffness is increased from 10 N/mm to 30 N/mm, the maximum additional spring force increases

by only 0.73 N, and the maximum variation ratio of the spring force increases by only 0.66%, as shown in Figs. 18 and 19, respectively.

V. CONCLUSIONS

The effects of structure parameters on the abnormal opening of the PRV under alternating pressure were investigated by numerical simulations. The following primary conclusions were drawn:

(1) The diameters of orifices 1 and 2 had a significant influence on the abnormal opening of the PRV under alternating pressure and were embodied in the form of coupling effect. The abnormal opening degree of the PRV was monotonously reduced by increasing the orifice 1 diameter. The influence of the orifice 2 diameter on the abnormal opening was dependent on the orifice 1 diameter. The reasonable diameters of orifices 1 and 2 are in the range of 0.8–1.2 mm.

(2) The volumes of the pilot valve inlet and the main valve spring chamber significantly affected the abnormal opening of the PRV by directly varying the pressure build-up rate in each chamber. When they decreased, the abnormal opening of the valve decreased significantly. The influence of the main valve spring chamber volume on the abnormal opening was more significant than the pilot valve inlet volume.

(3) The area ratio of the main spool and the main spring pre-compression force had similar effects on the abnormal opening, and their increase caused the abnormal opening to decrease linearly. However, their effects on the abnormal opening were not as significant as the first four analyzed parameters (d_1, d_2, V_1, and V_2), because of the structural constraints of the valve.

(4) Because of the negligible displacement of the main spool, the main spring stiffness had no significant effect on the abnormal opening of the PRV under alternating pressure.

NOMENCLATURE

p_0	pressure in main valve inlet (Pa)
p_1	pressure in pilot valve inlet (Pa)
p_2	pressure in main valve spring chamber (Pa)
p_T	pressure in main valve outlet (Pa)
q_0	flow rate through main valve inlet (m^3/s)
q_1	flow rate through orifice 1 (m^3/s)
q_2	flow rate through orifice 2 (m^3/s)
q_3	flow rate through pilot valve inlet (m^3/s)
q_m	flow rate through main valve outlet (m^3/s)
q_p	flow rate through pilot valve outlet (m^3/s)
d_0	diameter of drain hole on main valve sleeve (m)
d_1	diameter of orifice 1 (m)
d_2	diameter of orifice 2 (m)
d_3	diameter of orifice in pilot valve seat (m)
V_0	volume of main valve inlet (m^3)
V_1	volume of pilot valve inlet (m^3)
V_2	volume of main valve spring chamber (m^3)
n	number of drain holes on main valve sleeve
A_x	flow area of main valve outlet (m^2)
A_0	effective area of lower-end of main spool (m^2)
A_2	effective area of upper-end of main spool (m^2)
λ	area ratio of main spool
m_0	mass of main spool (kg)
m_1	mass of pilot spool (kg)
B_0	viscous damping coefficient of main spool (Ns/m)
B_1	viscous damping coefficient of pilot spool (Ns/m)
k_x	main spring stiffness (N/m)
k_y	pilot spring stiffness (N/m)
x_0	pre-compression displacement of main spring (m)
x	displacement of main spool (m)
y_0	pre-compression displacement of pilot spring (m)
y	displacement of pilot spool (m)
F_f	static friction between main spool and seat (N)
Fx_0	pre-compression force of main spring (N)
Fy_0	pre-compression force of pilot spring (N)
$C_{d,1}$	discharge coefficient of orifice 1
$C_{d,2}$	discharge coefficient of orifice 2
$C_{d,m}$	discharge coefficient of main valve port
$C_{d,p}$	discharge coefficient of pilot valve port
α	half cone angle of pilot spool (deg)
β	oil bulk modulus (Pa)
ρ	oil density (kg/m^3)

REFERENCES

[1] Y. Liu, G.-F. Gong, H.-Y. Yang, D. Han, and X.-L. Yang, "Mechanism of electro-hydraulic exciter for new tamping device," *J. Central South Univ.*, vol. 21, no. 2, pp. 511–520, 2014.

[2] H. Wang, G.-F. Gong, H.-B. Zhou, W. Wang, and Y. Liu, "A rotary valve controlled electro-hydraulic vibration exciter," *Proc. Inst. Mech. Eng. C, J. Mech. Eng. Sci.*, vol. 230, no. 19, pp. 3397–3407, 2015.

[3] W.-A. Jia, J. Ruan, and Y. Ren, "Separate control of high frequency electro-hydraulic vibration exciter," *Chin. J. Mech. Eng.*, vol. 24, no. 2, pp. 293–302, 2011.

[4] Y. Ren and J. Ruan, "Theoretical and experimental investigations of vibration waveforms excited by an electro-hydraulic type exciter for fatigue with a two-dimensional rotary valve," *Mechatronics*, vol. 33, pp. 161–172, Feb. 2016.

[5] X. Wang, W.-R. Wu, and Q.-H. Hao, "Analysis on response characteristics of counterbalanced valve in vibration system," *J. Eng. Stud.*, vol. 10, no. 2, pp. 199–205, 2018. [Online]. Available: http://en.cnki.com.cn/Article_en/CJFDTotal-GCKG201802011.htm

[6] W.-R. Wu, G.-T. Tian, and Q.-H. Hao, "Analysis and optimization of abnormal opening of main port of relief valve under alternating pressure," *J. Huazhong Univ. Sci. Technol.*, vol. 46, no. 7, pp. 78–83, 2018.

[7] P.-S. Zung and M.-H. Perng, "Nonlinear dynamic model of a two-stage pressure relief valve for designers," *J. Dyn. Syst., Meas., Control*, vol. 124, no. 1, pp. 62–66, 2002.

[8] O. Gad, "Comprehensive nonlinear modeling of a pilot operated relief valve," *J. Dyn. Syst., Meas., Control*, vol. 135, no. 1, 2013, Art. no. 011011.

[9] K. Dasgupta and R. Karmakar, "Dynamic analysis of pilot operated pressure relief valve," *Simul. Model. Pract. Theory*, vol. 10, nos. 1–2, pp. 35–49, 2002.

[10] S. Dimitrov, "Investigation of static characteristics of pilot operated pressure relief valves," *Ann. Fac. Eng. Hunedoara-Int. J. Eng.*, vol. 11, no. 2, pp. 201–206, 2013.

[11] J. Liang, X.-H. Luo, Y.-S. Liu, X.-W. Li, and T.-L. Shi, "A numerical investigation in effects of inlet pressure fluctuations on the flow and cavitation characteristics inside water hydraulic poppet valves," *Int. J. Heat Mass Transf.*, vol. 103, pp. 684–700, Dec. 2016.

[12] H.-L. Ren and T. Wang, "Development and modeling of an electromagnetic energy harvester from pressure fluctuations," *Mechatronics*, vol. 49, pp. 36–45, Feb. 2018.

[13] S. Dimitrov, "Transient response of a pilot operated pressure relief valve with compensating control piston," *Ann. Fac. Eng. Hunedoara-Int. J. Eng.*, vol. 12, no. 1, pp. 227–232, 2014.
[14] K. Dasgupta and J. Watton, "Dynamic analysis of proportional solenoid controlled piloted relief valve by bondgraph," *Simul. Model. Pract. Theory*, vol. 13, no. 1, pp. 21–38, 2005.
[15] Y. C. Shin, "Static and dynamic characteristics of a two stage pilot relief valve," *J. Dyn. Syst., Meas., Control*, vol. 113, no. 2, pp. 280–288, 1991.
[16] T. Nakanishi, S. Hayashi, T. Hayase, A. Shirai, M. Jotatsu, and H. Kawamoto, "Numerical simulation of water hydraulic relief valve," in *Proc. Fourth JFPS Int. Symp. Fluid Power*, Tokyo, Japan, 1999, pp. 555–560.
[17] Y.-J. Deng and Z.-W. Liu, "Optimal design of pilot proportional relief valve's structural parameters in giant forging hydraulic press," in *Proc. ISDEA*, Hainan, China, Jan. 2012, pp. 412–416.
[18] K. Suzuki and E. Urata, "Development of a direct pressure-sensing water hydraulic relief valve," *Int. J. Fluid Power*, vol. 9, no. 2, pp. 5–13, 2008.
[19] Y.-P. Hu and D.-S. Liu, "Static characteristics of relief value with pilot G-Π bridge hydraulic resistances network," in *Proc. 5th JFPS Int. Symp. Fluid Power*, Nara, Japan, 2002, pp. 739–744.
[20] Y.-S. Liu, X.-J. Ren, D.-F. Wu, D.-L. Li, and X.-H. Li, "Simulation and analysis of a seawater hydraulic relief valve in deep-sea environment," *Ocean Eng.*, vol. 125, pp. 182–190, Oct. 2016.
[21] O. Gad, "Bond graph modeling of a two-stage pressure relief valve," *J. Dyn. Syst., Meas., Control*, vol. 135, no. 4, pp. 41001–41012, 2013.
[22] R. Maiti, R. Saha, and J. Watton, "The static and dynamic characteristics of a pressure relief valve with a proportional solenoid-controlled pilot stage," *Proc. Inst. Mech. Eng. I, J. Syst. Control Eng.*, vol. 216, no. 2, pp. 143–156, 2002.
[23] X.-H. Luo, X.-F. He, S.-P. Cao, and X. Ba, "Theoretical and experimental analysis of a one-stage water hydraulic relief valve with a one-way damper," *J. Pressure Vessel Technol.*, vol. 135, no. 6, pp. 612101–612106, 2013.

QIANHUA HAO was born in Hengyang, China, in 1987. He received the master's degree in mechanical engineering from the College of Mechanical and Electrical Engineering, Central South University, Changsha, China, in 2012, where he is currently pursuing the Ph.D. degree. He is currently a Lecturer in the School of Energy and Electromechanical Engineering, Hunan University of Humanities, Science and Technology. His research interests include electro-hydraulic vibration exciters, energy saving, and hydraulic valves for hydraulic vibration exciters.

WANRONG WU was born in Changde, China, in 1965. He received the B.E., M.E., and Ph.D. degrees in mechanical engineering from Central South University, Changsha, China, in 1986, 1993, and 1999, respectively, where he is currently a Professor and a Doctoral Tutor with the College of Mechanical and Electrical Engineering.

He has authored or co-authored more than 60 journal and conference papers, and he holds 20 patents. His research interests include fluid power components and systems, hydraulic vibration exciters, and smart control systems.

Dr. Wu is a member of the Fluid Transmission and Control Branch, Chinese Mechanical Engineering Society.

XIANGJING LIANG was born in Changsha, China, in 1987. He received the master's degree in mechanical engineering from the College of Mechanical and Electrical Engineering, Central South University, Changsha, in 2012, where he is currently pursuing the Ph.D. degree. His research interests include electro-hydraulic control for mobile machinery and energy saving in hydraulic systems.

ZHI LIU was born in Yueyang, China, in 1986. He received the master's degree in mechanical engineering from the Guangdong University of Technology, Guangzhou, China, in 2013. He is currently pursuing the Ph.D. degree with the College of Mechanical and Electrical Engineering, Central South University, Changsha, China.

His research interests include fluid power components and composite drilling tools.